Nuclear Physics A554 (1993) 593–619
North-Holland

NUCLEAR
PHYSICS A

Electromagnetic decays of excited hyperons (II)*

Yasuo Umino[1]
Department of Physics, State University of New York at Stony Brook, Stony Brook, NY 11794, USA

Fred Myhrer
Department of Physics and Astronomy, University of South Carolina, Columbia, SC 29208, USA

Received 14 July 1992
(Revised 15 September 1992)

Abstract: Excited negative-parity hyperon masses are calculated in a chiral bag model in which the pion and the kaon fields are treated as perturbations. We also calculate the hadronic widths of $\Lambda(1520)$ and $\Lambda(1405)$ as well as the coupling constants of the lightest $I=0$ excited hyperon to the meson-baryon channels, and discuss how the dispersive effects of the hadronic meson-baryon decay channels affect the excited hyperon masses. Meson-cloud corrections to the electromagnetic decay widths of the two lightest excited hyperons into ground states Λ^0 and Σ^0 are calculated within the same model and are found to be small. Our results strengthen the argument that predictions of these hyperon radiative decay widths provide an excellent test for various quark models of hadrons.

1. Introduction

With the anticipated completion of CEBAF and the proposed KAON laboratory, there has been a renewed interest in the study of low-lying excited hyperons. [1]) Although the existence of these hyperon states has been established for quite some time, [2]) their underlying quark structure is not yet well understood. One reason is our poor knowledge of the excited hyperon mass spectrum [3]) which introduces uncertainties when building models of hadrons. Another reason is that the measurements of transition amplitudes involving excited-hyperon states, which test model-dependent wavefunctions and transition operators, have not been made with sufficient accuracy. Theoretically, a relatively simple type of such transitions is the electromagnetic one since corresponding transition currents and thus, the operators, can, in principle, be constructed once the model lagrangian and assumptions about the hadron structure are specified. Fortunately, calculations of electromagnetic transition amplitudes between excited- and ground-state hyperons are found to be

Correspondence to: Dr. Y. Umino, NIKHEF-K Theorie Groep, Postbus 41882, 1009 DB Amsterdam, The Netherlands.

* This work is supported in parts by grants from the NSF and the U.S. Department of Energy under contract #DE-FG02-88ER40388.

[1] Present address: NIKHEF-K, Postbus 41882, 1009 DB Amsterdam, The Netherlands.

strongly model dependent [4-7]) and their measurements, which are being planned at CEBAF [8]), may help to determine the hyperon wavefunction composition and thereby put strong restrictions on possible phenomenological models of hadrons.

Hyperon resonances also play an important role in low-energy $\bar{K}N$ interactions which are characterized by the presence of coupled two-particle channels. The $\pi\Sigma$ channel can couple to the low-energy $\bar{K}N$ system with isospin $I=0$ whereas both the $\pi\Sigma$ and $\pi\Lambda$ channels are open when the $\bar{K}N$ system is coupled to $I=1$. The lightest hyperon resonance, $\Lambda(1405)$, plays a crucial role in understanding the properties of the K^- atoms and to determine the structure of this state is of prime importance in K^- atomic studies. It has long been speculated that the $\Lambda(1405)$, being close to the $\bar{K}N$ threshold, is a candidate for the K^-p bound-state interpretation [12-14]) however, a similar analysis has not been made for $\Lambda(1520)$. A cloudy bag model analysis (to be discussed later) of low-energy S-wave $\bar{K}N$ scattering shows that $\Lambda(1405)$ is mostly a meson-baryon bound state [12]). Also, in the bound-state approach to the hyperons in the Skyrme model [15]), $\Lambda(1405)$ emerges naturally as a bound state of the strangeness-carrying kaon and the SU(2) soliton. This suggests that $\Lambda(1405)$ might have a dominant molecular $q^4\bar{q}$ structure instead of being a pure qqq state. In an effective meson-baryon theory the mass and the width of $\Lambda(1405)$ may be reproduced in a simple coupled-channel K-matrix analysis of $\pi\Sigma$ scattering [2,16]). For further developments see e.g. Oades and Rasche [17]) and Williams, Ji and Cotanch [18]).

In contrast, both the NRQM [9,10]) and chiral-bag-model calculations [7,19]) find that the *lightest* $\Lambda^*(\frac{1}{2}^-)$ qqq state is almost mass degenerate with the *lightest* $\Lambda^*(\frac{3}{2}^-)$ qqq state. In addition, the non-relativistic quark model (NRQM) finds $\Lambda(1405)$ to be predominantly a three-quark (qqq) flavor singlet state [9,10]) whereas in bag models it is about an even mixture of flavor singlet and octet states [7,11]) The chiral bag model, like the cloudy bag model, has a specific coupling to the open hadronic channels through the meson cloud. An improved treatment of this meson cloud (i.e., a proper inclusion of dispersive effects of the hadronic widths) might explain the observed $\boldsymbol{L}\cdot\boldsymbol{S}$ splitting of the lowest $J^P=\frac{1}{2}^-$ and $\frac{3}{2}^-$ Λ^* states [20-23]), an effect we shall estimate within our model in this work. If the $\Lambda(1405)$ is a molecular (or quasi-bound $\bar{K}N/\pi\Sigma$) state, then a further and so far un-observed low-lying three-quark $\Lambda^*(\frac{1}{2}^-)$ state should exist. Thus, establishing all the low-lying excited hyperons and probing the quark substructure of these hyperon resonances through, for example, their radiative transition rates will contribute towards a better understanding of the nature of the $\Lambda(1405)$ state and its role in low-energy $\bar{K}N$ interactions.

In two previous articles [7,19]) we calculated the masses and wavefunctions of the low-lying negative-parity baryon resonances as well as some hyperon radiative decay widths relevant to a planned CEBAF experiment [8]) using a perturbative version of the chiral bag model. In calculating the excited baryon masses we found that both the one-gluon exchange interactions and the dispersive effects from the pion-baryon channels play important roles in describing the mass spectrum [see ref. [7]) for errata

to tables 4 and 5 of ref. [19]). Errata to the figures and other tables of ref. [19]) are available upon request.]

In this paper we extend our work to include the kaon cloud in our model calculation of the hyperon mass spectrum and also estimate the effects due to mass differences between initial/final and intermediate baryons in the evaluation of baryon self-energy diagrams. Furthermore, in ref. [7]) we calculated only the quark core contributions to the radiative decay widths of $\Lambda(1520)$ and $\Lambda(1405)$ decaying into ground states Λ and Σ^0. These decay widths were found to be much smaller than those calculated in the NRQM [4]), due to the different spin-flavor content of excited hyperons in the two models. For example, the chiral bag model predicts, similar to the early but incomplete MIT bag calculations of these states [11]), a large but non-dominant admixture of flavor octet component in $\Lambda(1405)$, a state which has traditionally been treated as a flavor-singlet state based on the results of NRQM calculations [9,10]). This octet admixture reduces drastically the radiative decay widths of the lightest $\Lambda^*(\frac{1}{2}^-)$ state. The small hyperon radiative decay widths found in ref. [7]) imply that meson-cloud corrections to the model might affect the calculated widths, and therefore we calculate in this work the meson-cloud corrections to the above decays widths.

This paper is organized as follows. In the following section we present the excited-hyperon mass spectrum calculated with the kaon fields included in the meson cloud. We discuss how the dispersive effects of our calculated hadronic widths contribute to the hyperon masses and examine some of the difficulties encountered in evaluating the meson-cloud contributions to excited-baryon masses. The strong decay widths and coupling constants of $\Lambda(1520)$ and $\Lambda(1405)$ are then estimated with our model. In sect. 3 we present the meson-cloud corrections to the excited-hyperon radiative decay widths. Meson electromagnetic transition currents constructed to calculate these corrections are, in general, two-quark operators acting on spin-flavor wavefunctions of a three-quark system. Finally in sect. 4, we conclude with a summary and a discussion of the results of the present work.

2. Low-lying negative-parity hyperons

2.1. THE EXCITED-HYPERON MASS SPECTRUM

In this section we extend our calculation of the low-lying negative-parity hyperon mass spectrum by including the kaon-cloud contribution while neglecting the effects of the η-cloud. These massless meson fields are determined by a boundary condition on the bag surface requiring continuity of the axial current and are excluded from the bag interior so that chiral symmetry is realized in the Wigner-Weyl mode inside the bag and in the Nambu-Goldstone mode outside. As in ref. [7]), we use an approximation of the chiral bag model [24]) where the mesonic cloud surrounding the quark core is treated as a perturbation, giving our model lagrangian to lowest

order in the meson fields as

$$\mathscr{L}_{\text{Bag}} = \left[\left(i\bar{q}(x)\partial q(x) - \tfrac{1}{4}\sum_a F^a_{\mu\nu}(x)F^{\mu\nu a}(x) - B\right)\right]\theta_{\text{V}}$$

$$-\tfrac{1}{2}\bar{q}(x)\left[1+\frac{i}{f}\boldsymbol{\lambda}\cdot\boldsymbol{\phi}(x)\gamma_5\right]q(x)\delta_{\text{S}} + \tfrac{1}{2}(\partial_\mu\boldsymbol{\phi}(x))^2\theta_{\bar{\text{V}}}, \qquad (1)$$

where $q(x)$ and $\boldsymbol{\phi}(x)$ are the quark and octet meson fields, respectively, and

$$\theta_{\text{V}} = \begin{cases} 1 & \text{if} \quad x \in \text{V} \\ 0 & \text{if} \quad x \notin \text{V}. \end{cases} \qquad (2)$$

$\theta_{\bar{\text{V}}}$ is the compliment of θ_{V}, f is the appropriate meson decay constant (in this work we use $f_{\text{K}} = 1.09 f_\pi$), and $\delta_{\text{S}} = \delta(|x| - R)$ couples the quarks to meson fields on the bag surface. We will also give masses to the quarks and thereby to the mesons in our calculations. We shall refer to the above lagrangian when constructing effective-meson electromagnetic transition operators in sect. 3.

The method we use to calculate the excited-baryon masses in our approximation of the chiral bag has been described in detail in refs. [19,25]). The extension of the model calculation to include the kaon cloud is straightforward. As discussed in refs. [19,25]), when calculating the effective-quark one-meson exchange diagrams, only those diagrams where the intermediate baryon state, $|\text{B}'\rangle$, is the *same* as the initial/final baryon state, $|\text{B}\rangle$, are included in the diagonalization of the hamiltonian and minimization of the energy [see fig. 1 of ref. [19])]. Contributions to the baryon masses from those diagrams where the intermediate baryon state is *different* from the initial/final baryon state are included as corrections *after* the diagonalization and minimization procedure. Consequently, when calculating the Λ^* and Σ^* masses *all* contributions from the kaon cloud are treated as perturbative corrections to the masses and will therefore not affect the hyperon wavefunctions obtained in ref. [7]).

Fig. 1 shows the spectrum of low-lying negative-parity hyperon resonances calculated in our model when only the pion field and when both the pion and kaon fields are included in the meson cloud. In the present calculation we consider contributions from all quark one-gluon and effective one-pion and one-kaon exchange interactions to the masses. Here, as in refs. [7,19,25]), we do not correct for possible mass differences between the initial/final and intermediate baryon states in the meson-cloud correction terms. In the following section and in appendix A we will discuss this particular mass-difference correction and present an application to the lowest Λ^* states. The bag parameters used to fit the spectrum are $B^{1/4} = 145$ MeV, $Z_0 = 0.25$, $\alpha_{\text{s}} = 1.5$ and $m_{\text{S}} = 250$ MeV, which are the same as in ref. [7]), where the meson cloud consists only of pions, except that the zero-point/center-of-mass energy parameter, Z_0, has been changed from 0.45 to 0.25. This change in Z_0 is necessary because the kaon cloud lowers the masses of all states by about 30 to 60 MeV relative to our results in ref. [7]) for a wide range of input parameters as exemplified in fig. 1. However, the wave functions of the excited-hyperon states shown in fig. 1 remain the same as those

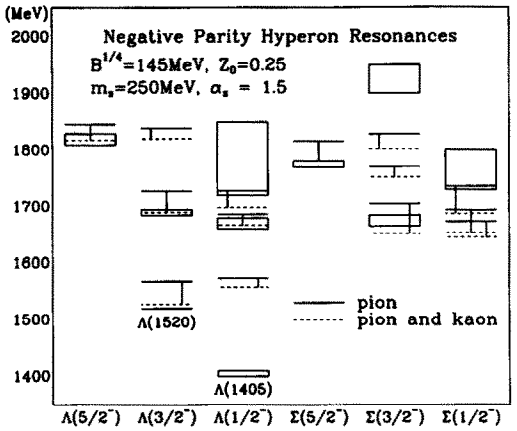

Fig. 1. The mass spectrum of the negative-parity Λ^* and Σ^* hyperons in the chiral bag model where the meson cloud is treated as perturbation. In the figure we show the observed hyperon resonances with their mass uncertainties taken from ref. [3]) and the calculated masses when (i) only the pion field (solid line) and (ii) both the pion and the kaon fields (dashed line) are included in the meson cloud. The vertical lines connect the same states *before* and *after* the kaon field has been included in the calculation. Note that when both the pion and kaon fields are included in the meson cloud, the mass of $\Sigma(\frac{5}{2}^-)$ state coincides with the upper limit of the $J^P = \frac{5}{2}^-\Sigma(1775)$ resonance.

obtained in ref. [7]), since a change in Z_0 only affects the diagonal elements of the bag hamiltonian. (The above change in Z_0 increases the stable bag radii by a few percent.)

It is instructive to compare our results with that of the NRQM calculation by Isgur and Karl [9]). Table 1 is a summary of the masses of low-lying negative-parity hyperons predicted in the NRQM and in our model together with the observed states. With the exception of $\Lambda(1405)$ to be discussed below, both models can reproduce the established hyperon resonances reasonably well and give similar

TABLE 1

Masses in MeV of low-lying negative-parity hyperon resonances calculated in the NRQM of ref. [9]) and in the chiral bag model in this work. The bag parameters used to calculate the entries in columns three and seven are $B^{1/4} = 145$ MeV, $Z_0 = 0.25$, $\alpha_s = 1.5$ and $m_S = 250$ MeV. The fourth and the eighth columns show the corresponding observed states taken from ref. [3])

State	NRQM	Chiral bag	Observed state	State	NRQM	Chiral bag	Observed state
$\Lambda(\frac{5}{2}^-)$	1815	1818	1810–1830	$\Sigma(\frac{5}{2}^-)$	1760	1780	1770–1780
$\Lambda(\frac{3}{2}^-)_1$	1880	1821	none	$\Sigma(\frac{3}{2}^-)_1$	1815	1802	none
$\Lambda(\frac{3}{2}^-)_2$	1690	1686	1685–1695	$\Sigma(\frac{3}{2}^-)_2$	1805	1752	none
$\Lambda(\frac{3}{2}^-)_3$	1490	1528	1518.5–1520.5	$\Sigma(\frac{3}{2}^-)_3$	1675	1651	1665–1685
$\Lambda(\frac{1}{2}^-)_1$	1800	1698	1720–1850	$\Sigma(\frac{1}{2}^-)_1$	1810	1688	1730–1800
$\Lambda(\frac{1}{2}^-)_2$	1650	1667	1660–1680	$\Sigma(\frac{1}{2}^-)_2$	1750	1653	none
$\Lambda(\frac{1}{2}^-)_3$	1490	1557	1400–1410	$\Sigma(\frac{1}{2}^-)_3$	1650	1645	none

predictions for states that have not been seen. In particular, they are successful in describing the ordering of the $J^P = \frac{5}{2}^- \Lambda^*$ and Σ^* states correctly as well as the mass splitting between the $J^P = \frac{3}{2}^-$ $\Lambda(1520)$ and $\Lambda(1690)$. In the Σ^* sector the states are not yet well determined experimentally but both models predict states near 1800 MeV and 1650 MeV with quantum numbers $J^P = \frac{3}{2}^-$ and $\frac{1}{2}^-$, respectively. However, from table 1 alone it is clear that the calculated hyperon states cannot be unambiguously identified with the observed resonances in the $I = 1$ sector.

Although both the NRQM and the chiral bag model predict similar masses for the negative-parity hyperon resonances, their wavefunctions are very different as shown in table 2, which lists the model predictions for spin-flavor contents of the excited hyperons in percents. (Note that in both models the $J^P = \frac{5}{2}^- \Lambda^*$ and Σ^* are pure spin-quartet, flavor-octet states.) Since the chiral bag model predicts an excited-hyperon mass spectrum very similar to the NRQM the differences in the predictions for the spin-flavor contents of these hyperon resonances between the two models become important and should be explored experimentally as discussed in refs. [6,7]).

2.2. A MODIFIED MESON-CLOUD CORRECTION

The most conspicuous state that both the NRQM and the above chiral-bag-model calculation fail to reproduce is the $J^P = \frac{1}{2}^- \Lambda(1405)$ state, a possible $\bar{K}N$ bound state mentioned in the Introduction. Recall that the NRQM predicts the lightest $J^P = \frac{1}{2}^-$

TABLE 2

Relative percentages of spin-flavor contents of low-lying negative-parity hyperons in the NRQM of ref. [9]) and in the chiral bag model of this work. The composition for $\Sigma(\frac{3}{2}^-)_2$ state in NRQM was not given in ref. [9]). In both models the $J^P = \frac{5}{2}^-$ hyperons are pure spin-quartet, flavor-octet states

Spin-flavor state	NRQM (in %)			Chiral bag (in %)		
	$\|^2 1\rangle$	$\|^4 8\rangle$	$\|^2 8\rangle$	$\|^2 1\rangle$	$\|^4 8\rangle$	$\|^2 8\rangle$
$\Lambda(\frac{3}{2}^-)_1$	0.2	98.0	1.2	0.0	85.7	14.2
$\Lambda(\frac{3}{2}^-)_2$	16.0	1.4	82.8	9.8	13.6	76.6
$\Lambda(\frac{3}{2}^-)_3$	82.8	0.0	16.0	90.5	0.9	8.7
$\Lambda(\frac{1}{2}^-)_1$	3.2	72.3	25.0	3.1	92.1	4.7
$\Lambda(\frac{1}{2}^-)_2$	15.2	33.6	56.2	37.4	7.7	54.8
$\Lambda(\frac{1}{2}^-)_3$	81.0	0.4	18.5	59.5	0.0	40.5
	$\|^2 10\rangle$	$\|^4 8\rangle$	$\|^2 8\rangle$	$\|^2 10\rangle$	$\|^4 8\rangle$	$\|^2 8\rangle$
$\Sigma(\frac{3}{2}^-)_1$	36.0	57.8	6.3	73.9	17.0	9.1
$\Sigma(\frac{3}{2}^-)_2$				25.7	63.3	11.1
$\Sigma(\frac{3}{2}^-)_3$	6.8	1.2	92.2	0.9	19.0	80.1
$\Sigma(\frac{1}{2}^-)_1$	84.6	4.4	10.9	91.1	2.4	6.5
$\Sigma(\frac{1}{2}^-)_2$	12.3	65.6	21.2	0.6	48.7	50.8
$\Sigma(\frac{1}{2}^-)_3$	2.9	29.2	67.2	8.3	48.8	43.0

and $\frac{3}{2}^{-}\Lambda^{*}$ states to be mass-degenerate and our model gives almost the same mass for these two states as well. In our model, the meson-cloud contributions to baryon masses correspond to evaluating baryon self-energy diagrams in which the initial baryon state couples to allowed intermediate meson–baryon channels. As mentioned above, it is necessary to correct these self-energy diagrams for possible mass differerences between the initial/final and intermediate baryon states. Therefore, we present here meson-cloud corrections which are modified by the mass-corrected dispersive effects and explore whether it can explain the observed mass splitting between $\Lambda(1520)$ and $\Lambda(1405)$.

The mass-difference corrections to baryon self-energy diagrams have been calculated in the chiral bag model within the perturbative meson-cloud approximation for the ground-state baryon masses [26]) using an effective Yukawa model [27]). In our calculations, the meson-cloud contribution to the baryon masses, i.e., the effective-quark one-meson exchange interaction matrix element, Σ_{B}, is written as [26])

$$\Sigma_{\mathrm{B}} = \sum_{i,j} \langle \mathrm{B}|O(i)O(j)|\mathrm{B}\rangle = \sum_{\mathrm{B}'} \sum_{i,j} \langle \mathrm{B}|O(i)|\mathrm{B}'\rangle\langle \mathrm{B}'|O(j)|\mathrm{B}\rangle . \tag{3}$$

Here i and j are summed over the three quarks and the operator product $O(i)O(j)$ is the appropriate two-body (if $i \neq j$) one-meson exchange interaction operator which acts on quarks i and j in the spin–flavor space. Due to mass differences between the states $|\mathrm{B}\rangle$ and $|\mathrm{B}'\rangle$, each term in the above sum over B′ should be multiplied by the real part of a correction factor $\delta_L(\mathrm{BB}')$, which, in the static approximation, is given by

$$\delta_L(\mathrm{BB}') = \int_0^K \frac{\mathrm{d}q\, q^{2(L+1)}}{\omega(\omega + m_{\mathrm{B}'} - m_{\mathrm{B}} - i\varepsilon)} \Big/ \int_0^K \frac{\mathrm{d}q\, q^{2(L+1)}}{\omega^2} . \tag{4}$$

Here $\omega = \sqrt{\mu^2 + q^2}$ where q is the meson momentum and μ is the meson mass. The momentum K ($\sim$500 MeV) [26]) is a cut-off reflecting the finite size of the source of the meson fields and is determined by the normalization integral appearing in the denominator of eq. (4). In the static approximation, K is of the order of $1/R$ where R is the bag radius. For the non-static case, the expression $\omega + m_{\mathrm{B}'} - m_{\mathrm{B}} - i\varepsilon$ in eq. (4) should be replaced by $\omega + \sqrt{m_{\mathrm{B}'}^2 + q^2} - m_{\mathrm{B}} - i\varepsilon$, and in our estimate we use the same normalization as in the static case. The relative intermediate meson–baryon angular momentum L has the values of $L = 0$ for $\mathrm{B} = \Lambda(\frac{1}{2}^{-})$ and $L = 2$ for $\mathrm{B} = \Lambda(\frac{3}{2}^{-})$ in our calculations. In this effective Yukawa model, the imaginary part of $\delta_L(\mathrm{BB}')$ gives the hadronic decay width of the baryon B.

The sum over intermediate baryon states $|\mathrm{B}'\rangle$ in eq. (3) should, in principle, include all the observed baryon states in the allowed meson–baryon channels for a given initial state $|\mathrm{B}\rangle$. The ground-state baryons are described by restricting the quarks to occupy only the lowest S-state. In this case, almost all contributions to the baryon self-energy diagrams come from octet and decuplet intermediate baryon ground states because higher excited $|\mathrm{B}'\rangle$ state contributions are negligible due to the large

mass differences $m_{B'} - m_B$. Therefore when $|B\rangle$ are the ground-state baryons (i.e. when quarks occupy only the S-states), their self-energies may be evaluated by considering only the ground-state intermediate states, and in such a case there are no ambiguities in assigning wavefunctions to each intermediate state $|B'\rangle$. Using this prescription Myhrer, Brown and Xu [26]) have found that the real part of multiplicative correction factors, Re $\delta_L(BB')$, are close to unity resulting in small corrections to baryon self-energies and help to improve the fit to the ground-state baryon mass spectrum.

However, if the initial and final baryon state is an excited state, it becomes necessary to include both ground state and excited baryon states in $|B'\rangle$, and this method runs into difficulties of a practical nature. Even when we limit $|B'\rangle$ to the quark space of either all three quarks in the lowest S-state or two in the lowest S-state and one in the lowest P-state ($P_{1/2}$ or $P_{3/2}$), difficulties arise in the choice of the calculated wavefunctions to be used in $|B'\rangle$. For example, consider contributions from the one-pion exchange interaction to the mass of Λ^*. In this case possible intermediate baryon states are the isospin-one Σ and their excited states, and the Σ^* wavefunctions are needed to evaluate each term in the one-pion exchange interaction matrix element, Σ_B. However, as shown in fig. 1, the Σ^* mass spectrum is very poorly known experimentally [3]) and many states predicted by quark models are not seen. This makes it very difficult to assign calculated negative-parity Σ^* wavefunctions to observed resonances and contributes to the theoretical uncertainty in the resulting Λ^* mass. Another example of practical difficulties arises in calculating the mass corrections due to the one-K^+ exchange. This requires knowledge of our model wavefunctions for the low-lying negative-parity Ξ^- states which we have not yet calculated. Because of these difficulties, we chose to ignore corrections due to mass differences between the initial/final and intermediate baryon states when we calculate the baryon self-energy contributions to the overall excited-hyperon mass spectrum discussed in sect. 2.1 and shown in fig. 1. Again, note that because the mass-difference corrections apply only to those one-meson exchange diagrams where the intermediate baryon state is *different* from the initial/final baryon state, they do not affect our calculated wavefunctions of excited hyperons which are used in sect. 3.

We shall now make a very restricted application of the above mass corrections to see if a better treatment of the meson–baryon channels in the baryon self-energy diagrams might contribute to an understanding of the mass splitting between $\Lambda(1520)$ and $\Lambda(1405)$. The lightest $\Lambda(\frac{3}{2}^-)$ and $\Lambda(\frac{1}{2}^-)$ states are identified with $\Lambda(1520)$ and $\Lambda(1405)$ and are denoted in table 1 as $\Lambda(\frac{3}{2}^-)_3$ and $\Lambda(\frac{1}{2}^-)_3$, respectively. We shall estimate the magnitude of mass corrections in the spirit of the work by Arima and Yazaki [21]). They investigated the problem of mass splitting between $\Lambda(1520)$ and $\Lambda(1405)$ using a NRQM with mesonic degrees of freedom, assuming that the two states have equal "bare" masses. In this effective meson–baryon model the hyperons acquire their physical masses through the coupling to the meson–baryon channels. They found that in order to generate a low mass for the lightest $J^P = \frac{1}{2}^- \Lambda^*$ state

relative to the $\frac{3}{2}^-$ state, it was necessary to introduce strong couplings to the intermediate $\bar{K}N$ and $\pi\Sigma$ channel. This is also similar in spirit to the work in the cloudy bag model [12]) which unfortunately was limited to $\Lambda(1405)$ only. We consider it very important to describe simultaneously both $\Lambda(1520)$ and $\Lambda(1405)$ in any model of baryons since the coupling in the $J^P = \frac{1}{2}^-$ and $\frac{3}{2}^-$ channels are linked and both states couple to the $\pi\Sigma$ and $\bar{K}N$ meson-baryon channels. When we consider the pure-hyperon three-quark states including one-gluon exchange corrections, we find that the two lightest $\Lambda(\frac{3}{2}^-)$ and $\Lambda(\frac{1}{2}^-)$ states are almost mass degenerate [7]), which is the assumption made by Arima and Yazaki [21]). We find that the masses for these states remain nearly degenerate when the pion cloud is included [7]), but the kaon cloud lifts this mass degeneracy as seen in fig. 1 and discussed in appendix A. In our estimates we shall use Σ_B of eq. (3) with the real part of the correction factor of eq. (4) and consider only the case where $B = \Lambda^*$ and with all the intermediate quarks in the S-state. The ground-state N- and Δ-contributions have different masses due to the one-gluon exchange interaction, and to evaluate the largest corrections, we neglect the heavy $\bar{K}\Delta$ and $\pi\Sigma^*(1385)$ intermediate states in our estimate as in earlier calculations [12,20-22]). This means B′ includes only the octet baryons, i.e., $B' = N$ for the kaon cloud and $B' = \Sigma$ for the pion cloud. Since we are calculating the meson-cloud contribution to the hyperon masses, one should not use the physical B and B′ masses, but only their "bare" masses which include the gluonic mass corrections [26]) that exist even in the chiral limit. Additional details are given in appendix A.

Our model estimate confirms the findings of Arima and Yazaki [21]) that quark models with a qqq structure for hyperons have difficulties in explaining the $\Lambda(1520)$ and $\Lambda(1405)$ mass difference. Further examinations regarding the nature of $\Lambda(1405)$ are necessary, and we stress again that it is imperative to treat both $\Lambda(1405)$ and $\Lambda(1502)$ in the same model and then repeat, for example, the cloudy bag model calculation of Veit *et al.* [12]) starting with the "bare" masses of $\Lambda(1405)$ and $\Lambda(1520)$ about equal and use the coupling to the meson-baryon channels to get the observed hyperon masses. We note that the cloudy bag model allows for a quark-meson four-point interaction in the bag volume which generates an S-wave meson-baryon contact interaction. In their model this specific interaction, which is of second order in f_π^{-2} and is *not* included in our model, is responsible for the remarkable lowering of the $\Lambda(1405)$ mass. It would be interesting to investigate if this second-order quark-meson interaction will affect the mass of the $\Lambda(1520)$ equally strongly. Such an investigation might give us some further clues to the question of whether the quark content of $\Lambda(1405)$ differs from that of $\Lambda(1520)$ or not*. We find that although the "bare masses" (i.e. masses before meson-cloud corrections) of our two *lightest* $J^P = \frac{1}{2}^-$ and $\frac{3}{2}^-$ hyperon states are about equal (~1695 MeV with the bag parameters used in fig. 1), their flavor contents are different with $\Lambda(\frac{1}{2}^-)_3$ being almost equal mixtures of flavor-singlet and flavor-octet states (see table 2).

* In *all* of the cloudy bag model calculations, the $\Lambda(1405)$ is *assumed* to be a flavor-singlet state.

2.3. STRONG DECAY WIDTHS AND COUPLING CONSTANTS

In this subsection we estimate the hadronic decay widths of the two lightest excited hyperons, given by the imaginary part of eq. (4), and the coupling constants of $\Lambda(1405)$ into the meson-baryon channels. For the hadronic decay widths we use the observed physical mass differences and our "non-static" expression in eq. (4) to get the correct centrifugal factor, using a bag radius R of 1.2 fm and a strange quark mass m_S of 250 MeV. Also, as discussed in appendix A, we do not restrict the sum over the quark indices to the case $i \neq j$ in eq. (3). Then the hadronic decay width of $\Lambda(1520)$ into the $\pi\Sigma$ channel is given by

$$\Gamma_{\pi\Sigma}[\Lambda(1520)] = 5(\sqrt{\tfrac{1}{2}}\, a - \tfrac{1}{2}\sqrt{\tfrac{1}{5}}\, b - \tfrac{1}{2}c)^2 \times 7.7 \text{ MeV}. \tag{5}$$

Here the strength of the quadrupole transition operator k^{π}_{SAAS} of ref. [19]), table 2, is used to find the width. A similar quadrupole transition operator for the kaon cloud, $k^{K}_{SA'A'S}$, (A' indicates a massive s-quark in the $P_{3/2}$ state), is used to determine the hadronic width of $\Lambda(1520)$ into the $\bar{K}N$ channel which we find to be

$$\Gamma_{\bar{K}N}[\Lambda(1520)] = \tfrac{5}{2}(a + \sqrt{2}c)^2 \times 2.4 \text{ MeV}. \tag{6}$$

For $\Lambda(1405)$ the hadronic width is given by

$$\Gamma_{\pi\Sigma}[\Lambda(1405)] = (a' + \sqrt{\tfrac{1}{2}}\, b' - \sqrt{\tfrac{1}{2}}\, c')^2 \times 19.3 \text{ MeV}, \tag{7}$$

where the magnitude of the width is determined by the monopole transition operator for the pion cloud, m^{π}_{SPPS}, of ref. [19]). Here a, b, c and a', b', c' are the spin-flavor coefficients for the excited-hyperon wavefunctions in the jj coupled basis. For $\Lambda(1520)$ they are defined as

$$|\Lambda(1520)\rangle \equiv a|\mathbf{1};\, SSA\rangle' + b|\mathbf{8};\, SSA\rangle + c|\mathbf{8};\, SSA\rangle' + d|\mathbf{8};\, SSP\rangle, \tag{8}$$

where $S \equiv S_{1/2}$, $P \equiv P_{1/2}$ and $A \equiv P_{3/2}$, and the corresponding coefficients for $\Lambda(1405)$ are

$$|\Lambda(1405)\rangle \equiv a'|\mathbf{1};\, SSP\rangle' + b'|\mathbf{8};\, SSP\rangle' + c'|\mathbf{8};\, SSP\rangle' + d'|\mathbf{8};\, SSA\rangle. \tag{9}$$

Using the calculated wavefunctions for $\Lambda(1520)$ and $\Lambda(1405)$ given in eqs. (5) and (6) of ref. [7])* together with its appendix, one finds the following values for these coefficients:

$$a = +0.95, \quad b = -0.21, \quad c = +0.21, \quad d = 0.07, \tag{10}$$

$$a' = +0.77, \quad b' = +0.15, \quad c' = +0.45, \quad d' = -0.43. \tag{11}$$

With these values for the spin-flavor coefficients we find the total $\Lambda(1520)$ decay width to be 23.6 MeV compared to the measured width of 15.6 MeV [ref. [3])]. Note that if $\Lambda(1520)$ is a pure flavor-singlet state ($a = 1$, $b = 0$, $c = 0$ and $d = 0$) the relative branching ratio $\Gamma_{\pi\Sigma}[\Lambda(1520)]/\Gamma_{\bar{K}N}[\Lambda(1520)]$ increases from $14.4/9.2 \approx 1.6$ to

* Eq. (6) in ref. [7]) contains a misprint: 0.03 should be 0.003.

approximately $7.7/2.4 \approx 3.2$. For $\Lambda(1405)$ we find $\Gamma_{\pi\Sigma}[\Lambda(1405)] \approx 6$ MeV, whereas if $\Lambda(1405)$ is a pure flavor singlet then eq. (7) gives a width of about 19.3 MeV. We note that the values of these widths depend somewhat on the value of the bag radius R. For example, if $R = 1.175$ fm then the total widths for the $\Lambda(1520)$ decreases to 19 MeV, a value closer to the measured width, but $\Gamma_{\pi\Sigma}[\Lambda(1405)]$ changes only by 1 MeV to 5 MeV. The value of the $\Lambda(1405)$ width is difficult to extract from experimental data since this hyperon, a resonance only 27 MeV below the K^-p threshold, can only be seen in the $\pi\Sigma$ channel. However, our calculated hadronic width for $\Lambda(1405)$ are clearly too small, a result which will be reflected in a too small hadronic coupling constant as discussed in the following paragraph. The latest analysis of the experimental $\pi^-\Sigma^+$ mass spectrum by Dalitz and Deloff [28]) gives a value of 50 ± 2 MeV for this width.

The magnitude of the coupling constants for the hyperon Y* coupling to the $\bar{K}N$ and $\pi\Sigma$ channels can also be calculated in the chiral bag model. For $\Lambda(1405)$ we find the ratio of these coupling constants to be

$$\frac{G^2_{\Lambda(1405)\bar{K}N}}{G^2_{\Lambda(1405)\pi\Sigma}} = \frac{2}{3}\,\frac{m^K_{SP'P'S}}{m^\pi_{SPPS}}\,\frac{(a'+\sqrt{2}c')^2}{(a'+\sqrt{\tfrac{1}{2}}b'-\sqrt{\tfrac{1}{2}}c')^2}, \tag{12}$$

where $m^K_{SP'P'S}/m^\pi_{SPPS}$ is the ratio of the strength of the monopole transition operator for the kaon cloud to that of the pion cloud, which depends on R and m_S. (Similar to above, P' denotes a massive s-quark in the $P_{1/2}$ state.) In eq. (12) we use the same convention as in table 6.6 of the compilation by Dumbrajs *et al.* [29]) where $G^2_{\Lambda(1405)\pi\Sigma}$ is defined in their equation (6.4)*. Note that from eqs. (5), (6), (7) and (12) one sees that neither the $|\mathbf{8}; SSP\rangle$ component of $\Lambda(1520)$ nor the $|\mathbf{8}; SSA\rangle$ component of $\Lambda(1405)$ couple to the $\bar{K}N$ or the $\pi\Sigma$ channels. From eq. (12) it is clear that the ratio of the two $\Lambda(1405)$ coupling constants equals $\frac{2}{3}$ only if: (i) $\Lambda(1405)$ is a flavor singlet ($a' = 1$; $b' = c' = d' = 0$) and (ii) we are in the SU(3) limit where the pion and kaon masses as well as the u-, d- and s-quark masses are equal, so that the ratio $m^K_{SP'P'S}/m^\pi_{SPPS} = 1$. Otherwise, the ratio of the coupling constants will be different from $\frac{2}{3}$. The flavor-octet part of $\Lambda(1405)$ will increase the value of the ratio from $\frac{2}{3}$, whereas the meson-cloud corrections to this "bare" quark model value tend to make the ratio much smaller than $\frac{2}{3}$ due to the very different kaon and pion masses. With our values for the spin-flavor coefficients a', b' and c' given in eq. (11) we find the ratio of coupling constants in eq. (12) to be 4.3 in the SU(3) limit. Including the physical meson masses, which corresponds to $m^K_{SP'P'S}/m^\pi_{SPPS} \approx 0.11$ at $R = 1.2$ fm and $m_S = 250$ MeV, we find this ratio reduced to approximately 0.47. It would be very useful to reanalyze the $\bar{K}N$ scattering data to see if this ratio of coupling constants for $\Lambda(1405)$ is much smaller or larger than $\frac{2}{3}$. If one uses both table 6.6 in Dumbrajs *et al.* [29]) and table 6.14 of an earlier data analysis compilation

* The definitions of strong-coupling constants used in ref. [29]) are not always consistent. Also the footnote (a) to table 6.6 in this reference is incorrect. The ratio of coupling constants should *increase* if g^2 were used as correctly stated in footnote (a) of table 6.14 of Nagels *et al.* [30]).

by Nagels *et al.*, [30]) it is seen that even a small value for the ratio of the coupling constants is not ruled out. However, in our model the quark-meson coupling is at the bag surface, and the meson fields have a sharp cut-off, which is unphysical. Our meson-cloud contribution to the ratio $m^{K}_{SP'P'S}/m^{\pi}_{SPPS} \approx 0.11$ might therefore be unrealistic.

Using eq. (6.4) of Dumbrajs *et al.* [29]) and the value we found above for the hadronic width of $\Lambda(1405)$, the magnitude of the coupling constant $|G_{\Lambda(1405)\pi\Sigma}|$ is found to be 0.698 with $R = 1.2$ fm and $m_S = 250$ MeV. Here $G_{\Lambda(1405)\pi\Sigma}$ is the charge-independent coupling to the $\pi\Sigma$. The ratio $G^2_{\Lambda(1405)\bar{K}N}/G^2_{\Lambda(1405)\pi\Sigma} = 0.43$ then determines the coupling of $\Lambda(1405)$ to the $\bar{K}N$ channel, $|G_{\Lambda(1405)\bar{K}N}| = 0.46$. If $\Lambda(1405)$ were a pure flavor-singlet state, the magnitude of the $\Lambda(1405)\pi\Sigma$ coupling constant increases to $|G_{\Lambda(1405)\pi\Sigma}|_1 = 1.211$ while the corresponding coupling to the $\bar{K}N$ channel decreases to $|G_{\Lambda(1405)\bar{K}N}|_1 = 0.327$.

In addition to these coupling constants for $\Lambda(1405)$, we have also calculated the magnitude of the strong-coupling constants $G_{\Lambda\bar{K}N}$ and $G_{\Sigma^0\bar{K}N}$ within our model as shown in appendix B. These hyperon coupling constants are defined for each charge state to conform to the notation of table 6.3 and sect. 2.3 of Dumbrajs *et al.* [29]). With $R = 1.125$ fm for the Λ^* and Σ^* and $m_S = 250$ MeV, we find that the chiral bag model gives $|G_{\Lambda\bar{K}N}| = 9.68$ and $|G_{\Sigma^0\bar{K}N}| = 3.23$, values which are somewhat smaller than those quoted in table 6.3 of Dumbrajs *et al.* [29]). However, these values for $\Lambda\bar{K}N$ and $\Sigma^0\bar{K}N$ coupling constants are well within the range reported in a more recent compilation by Adelseck and Saghai [31]). We note that a recent calculation in the bound-state approach to the Skyrme model by Gobbi *et al.* gives $G_{\Lambda\bar{K}N} = -9.93$ and $G_{\Sigma^0\bar{K}N} = +3.43$ when evaluated with a pion-mass term in the model lagrangian [32]).

3. Hyperon radiative decay widths: Meson-cloud contribution

As stated above, it is not possible to distinguish the NRQM from the chiral bag model using the results presented in tables 1 and 2. Instead, one needs to compare calculated observables which are sensitive to the predicted hyperon wavefunctions of table 2. One such observable is the radiative decay widths of excited hyperons decaying into their ground states. In this section we use our simple two-phase model of baryons, described by the lagrangian in eq. (1), to extract meson transition electromagnetic currents and evaluate meson-cloud corrections to the total hyperon radiative decay widths.

Before presenting the details of the calculation it should be emphasized that in our model the quark-meson coupling at the bag surface, determined by the requirement of a continuous axial current in the chiral symmetry limit, is *pseudoscalar* implying that the photon only couples to the mesons through the kinetic energy term. Therefore, contributions to the meson electromagnetic current comes only from those diagrams where the photon couples to the mesons in flight as shown in

fig. 2c. The cloudy bag model [12]), uses, in addition to the four-point quark-meson interaction, a derivative quark-meson coupling in the bag volume. This means that the photon can couple to the mesons inside the quark core and allows for a quark-meson-photon contact interaction (figs. 2a and 2b). We ignore contributions to the decay widths from those diagrams shown in fig. 2d, where the intermediate baryon radiates a photon while the meson is in flight. In principle, this diagram should be included but its effect is small compared with the process shown in fig. 2c, roughly by the ratio of meson to baryon masses. As we shall show, the contribution from the diagram fig. 2c to the total hyperon radiative width is small and therefore ignoring fig. 2d will not have any numerical consequence in this calculation. This approximation is also invoked by Zhong *et al.* [33]) who used a chiral SU(3) version of the cloudy bag model to calculate the branching ratios of the K^-p atom. In their

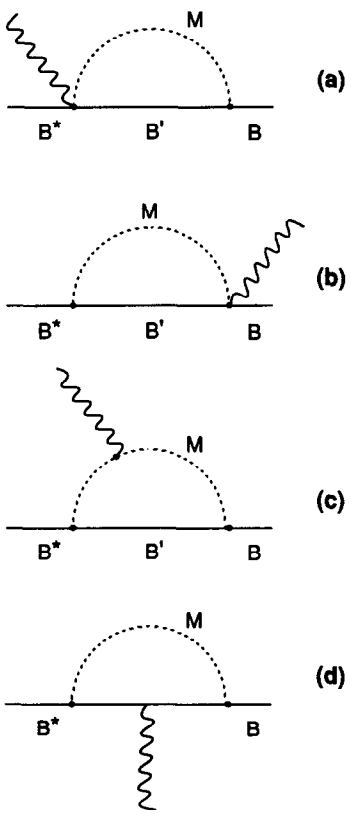

Fig. 2. (a) and (b): The quark-meson-photon contact interaction which is *absent* in a chiral bag model described by the lagrangian given in eq. (1) due to the *pseudoscalar* quark-meson coupling at the bag surface. (c): The only type of contribution to the meson electromagnetic transition current considered in this work. Here the photon (wiggly line) couples to the meson (dashed line) in flight. (d): Radiation of a photon from an intermediate baryon while the meson is in flight. Because the baryons are heavy compared to mesons this diagram has been omitted in the present work as well as in ref. [33]).

calculation, the $\Lambda(1405)$, which they assume to be a purely flavor-singlet state, gives a relatively small contribution to the radiative decay width of the K^-p atom. The reason is that $\bar{K}N$ atomic system is close to the $\bar{K}N$ threshold which is at the upper tail of the $\Lambda(1405)$ width, and the $\Lambda(1405)$ coupling strength is therefore considerably reduced in the atomic branching ratios.

Having defined the model lagrangian, meson electromagnetic transition currents can be extracted in the usual manner by introducing the minimal-coupling prescription $\partial_\mu \to \partial_\mu \pm ieA_\mu$. The total decay width receives contributions both from the quark core and the meson cloud and, using the notation of ref. [6]), is given by

$$\Gamma_{J_i J_f} = \frac{2k}{2J_i+1} \sum_{m_i m_f} \sum_{\lambda=\pm 1} |\langle J_f m_f | \hat{\varepsilon}^*_\lambda(\hat{k}) \cdot (\boldsymbol{I}_q + \boldsymbol{I}_m) | J_i m_i \rangle|^2 . \tag{13}$$

Here $\hat{\boldsymbol{\varepsilon}}$ is the photon polarization vector and $\boldsymbol{I}_q$ and $\boldsymbol{I}_m$ are defined as

$$\boldsymbol{I}_q \equiv \int_0^R d^3r \, \boldsymbol{J}_q(\boldsymbol{r}) \, e^{-i\boldsymbol{k}\cdot\boldsymbol{r}} , \tag{14}$$

$$\boldsymbol{I}_m \equiv \int_R^\infty d^3r \, \boldsymbol{J}_m(\boldsymbol{r}) \, e^{-i\boldsymbol{k}\cdot\boldsymbol{r}} , \tag{15}$$

where R is the bag radius. In eqs. (14) and (15), $\boldsymbol{J}_q$ and $\boldsymbol{J}_m$ are the quark and meson electromagnetic current operators, respectively, and, as in refs. [6,7]), we take the photon momentum k to be given by the observed mass difference between the initial and final hyperon states. The current $\boldsymbol{J}_m$ is generally a two-body operator such that the transition operator given in eq. (15) has the structure $\boldsymbol{I}_m = \sum_{i,j} O(i)O(j)$ which is similar to the effective-quark one-meson exchange interaction operator in eq. (3). Thus, for example, the meson-cloud contribution to the matrix element for the radiative decay of $\Lambda(1405)$ into Σ^0 is written as

$$\langle \Sigma^0 | \boldsymbol{I}_m | \Lambda(1405) \rangle = \sum_{B'} \sum_{i,j} \langle \Sigma^0 | O(i) | B' \rangle \langle B' | O(j) | \Lambda(1405) \rangle . \tag{16}$$

As a result, we are faced with the problem of the choice of wavefunctions for the intermediate baryon states, a problem similar to the one already addressed in the previous section. In this work we use only the ground-state octet and decuplet baryons with all three quarks in the S-state for intermediate $|B'\rangle$ states and, as a first approximation, neglect baryon mass differences as well as recoil corrections. This means the possible intermediate baryon states included in eq. (16) are $B' = p$, Ξ^-, Σ^+, Σ^-, Δ^+, Ξ^{-*}, Σ^{+*} and Σ^{-*}. In appendix C we present some explicit examples of the meson electromagnetic currents, $\boldsymbol{J}_m$, and give expressions for the corresponding transition operators $\boldsymbol{I}_m$.

We find that contributions from $\pi^+\Sigma^-$ and $\pi^-\Sigma^+$ as well as $\pi^+\Sigma^{-*}$ and $\pi^-\Sigma^{+*}$ intermediate states cancel each other when evaluating the matrix element $\langle \Lambda | \boldsymbol{I}_m | \Lambda^* \rangle$ for the radiative decay of Λ^* into $\Lambda\gamma$. The reason is that the strong-coupling constants

for the processes $\pi^-\Sigma^+ \to \Lambda$ and $\pi^+\Sigma^- \to \Lambda$ (as well as $\pi^\pm\Sigma^\mp \to \Lambda^*$) have the *same* sign whereas the π^+ and π^- transition electromagnetic currents connecting the states Λ^* and Λ have the *opposite* sign thus cancelling the contributions from $\pi^+\Sigma^-$ and $\pi^-\Sigma^+$ intermediate states in the matrix element for the radiative widths. Consequently, in this model, the pions are effectively spectators for $\Lambda^* \to \Lambda\gamma$ decays in contrast to $\Lambda^* \to \Sigma^0\gamma$ decays where both the kaon and pion clouds contribute to the total decay widths. Furthermore, there are no contributions from the $K^-\Delta^+$ intermediate state to the radiative decays of $\Lambda(1520)$ and $\Lambda(1405)$ for the following reason. If the initial excited hyperon is to radiate through the K^- cloud, a strange quark must initially be in an excited state implying that both the u- and d-quarks are in S-states and form an antisymmetric spin-flavor state. Therefore, the initial hyperon state cannot couple to the Δ^+ intermediate state with a totally symmetric spin-flavor wavefunction.

The results of our calculations are summarized in table 3 where we present the separate incoherent quark core and meson-cloud contributions as well as the total hyperon radiative decay widths. As in ref. [7]), we use $m_S = 250$ MeV and $R = 1.125$ fm to calculate these widths. It is clear that the meson-cloud corrections to the decay widths are negligible except in the case of the decay $\Lambda(1405) \to \Sigma^0 + \gamma$ where the width decreases from 2.22 to 1.85 keV when the meson-cloud corrections are included. The meson-cloud contributions to the widths for the decay process $\Lambda^* \to \Lambda + \gamma$ is much smaller than those for $\Lambda^* \to \Sigma^0 + \gamma$ decays as expected due to the heavy kaon mass, i.e., the meson-cloud contributions to the radiative decay widths, though small, come from the pion cloud.

These results are a direct consequence of the weak meson field approximation to the chiral bag model. In this approximation, the meson fields are localized just outside the bag surface and their strength decreases very rapidly as one moves away from the quark source on the surface. Numerically, the smallness of the meson-cloud contributions come from the small values of integrals I_1 to I_6 defined in eqs. (C.17) to (C.22) in appendix C. These are small due to the damping factor of $e^{-2\mu Rx}$

TABLE 3

Hyperon radiative decay widths in keV in the linearized approximation to the chiral bag model. In columns two and three we show the separated incoherent parts of the quark core (Γ_q) and meson cloud (Γ_m) contributions to the decay width. The total decay widths defined in eq. (13) is shown in the fourth column. As in ref. [7]) we use $m_S = 250$ MeV and $R = 1.125$ fm to calculate the widths.

Transition	Γ_q	Γ_m	Γ_{total}
$\Gamma(\Lambda(1520) \to \Lambda^0 + \gamma)$	31.60	3×10^{-3}	31.46
$\Gamma(\Lambda(1520) \to \Sigma^0 + \gamma)$	48.83	0.33	50.85
$\Gamma(\Lambda(1405) \to \Lambda^0 + \gamma)$	75.15	7×10^{-4}	74.98
$\Gamma(\Lambda(1405) \to \Sigma^0 + \gamma)$	2.22	0.04	1.85

appearing in the integrands, which means only the region near the (sharp) bag surface contribute to the integrals. In fact, this can be seen in the radial charge density of the Λ, calculated in the cloudy bag model by Kunz, Mulders and Miller [34]). They find a vanishing charge density at a distance of about 0.5 fm outside the bag cavity [see fig. 2 of ref. [34])]. This situation is similar to the description of excited Λ in our model although the two models will probably disagree in their predictions of the radiative decay widths due to different meson-photon couplings.

4. Discussion and conclusion

In this work we have calculated the masses of low-lying negative-parity hyperons in a perturbative approximation to the chiral bag model incorporating both pion and kaon fields in the meson cloud and found that the resulting mass spectrum is very similar to the one predicted by the NRQM calculation of Isgur and Karl [9]). Not only do both models reproduce this mass spectrum to some extent, but they also predict yet unobserved states sharing the same quantum numbers. However, both models fail to reproduce the observed mass splitting between $\Lambda(1520)$ and $\Lambda(1405)$. Without the kaon cloud, our model, like the NRQM, finds the lightest $J^P = \frac{3}{2}^-$ and $\frac{1}{2}^-$ Λ^* states to be degenerate in mass. A more careful treatment of the baryon self-energy diagrams takes the mass difference between the initial/final and the intermediate baryons into consideration. An estimate of this mass-difference correction indicates that it is the large flavor-singlet component in the $\Lambda(1520)$ which lowers its mass below that of $\Lambda(1405)$ when the kaon cloud is included in our model.

We have also calculated the hadronic widths of $\Lambda(1520)$ and $\Lambda(1405)$ and found that the total width of $\Lambda(1520)$ agrees well with experiment whereas the prediction for the $\Lambda(1405)$ width is too small relative to the currently accepted value. If we include the effects of the kaon and pion clouds, the ratio of the square of coupling constants of $\Lambda(1405)$ coupling to the $\bar{K}N$ and $\pi\Sigma$ channels was also found to be small compared to most data analysis [29,30]). We find in this paper that the chiral bag model gives values for the ΛKN and the $\Sigma^0 KN$ coupling constants consistent with the latest compilation by Adelseck and Saghai [31]) and the Skyrme model calculation by Gobbi *et al.* [32]) In view of this it seems like our dominant qqq assumption regarding $\Lambda(1405)$ has some difficulties. However, we note that the only reliable quantity in an analysis of $\Lambda(1405)$ is the strength of the residue at the $\Lambda(1405)$ pole which can only be reached via a dispersion calculation analysis of the experimental data. Current $\bar{K}N$ and $\pi\Sigma$ scattering data are too crude to allow for a reliable dispersion analysis.

In addition to the hadronic widths of the lightest $J^P = \frac{3}{2}^-$ and $\frac{1}{2}^-$ hyperons, we evaluated the meson-cloud corrections to the radiative decay widths of $\Lambda(1520)$ and $\Lambda(1405)$ which we claim to be a very good observable to test various models of hadrons. In our model the radiative decay of an excited hyperon proceeds mainly

through the radiation of a photon by the excited valence quarks and almost no radiation occurs from the meson cloud. To examine this further, one should calculate the excited-baryon mass spectra with the non-perturbative (topological) chiral bag model [35]), which is technically very challenging. The model we use in this work is the weak meson field approximation to the topological bag model, which enhances the role of the quarks in the bag cavity while ignoring the non-perturbative effects of the meson cloud. Another extreme approximation to the topological bag model is the soliton description of baryons without any explicit quark degrees of freedom. The Skyrme model is a prototype of such soliton models of baryons, and hyperon resonances have been studied using this model [36]). A calculation of the radiative decay widths of excited hyperons in the Skyrme model for comparison with predictions from models of baryons containing explicit quark degrees of freedom is currently in progress by one of the authors [37]).

In ref. [38]), Burkhardt and Lowe extract the radiative decay widths of $\Lambda(1405)$ decaying into ground states Σ^0 and Λ using the measured branching ratios for the radiative decay of the K^-p atom [39]) They use a pole model to calculate the K^-p atom radiative decay branching ratios in order to determine the $\Lambda(1405)$ radiative decay widths. The $\Lambda(1405)$ coupling constant to the $\bar{K}N$ channel and the $\Lambda\bar{K}N$ and $\Sigma^0\bar{K}N$ coupling constants are among the input parameters of this analysis. We find a small value of the $\Lambda(1405)\bar{K}N$ coupling constant, a reflection of the small $\Lambda(1405)$ hadronic widths obtained through eq. (7). A pole model analysis with this small coupling gives $\Lambda(1405)$ radiative decay widths larger than predictions reported in the literature [40]). This together with our unsuccessful attempt in obtaining a $\Lambda(1520)$ and $\Lambda(1405)$ mass splitting and with the cloudy bag model results of going to the next order in the meson-field coupling, indicate that the $\Lambda(1405)$ structure is more than a simple three-quark state. In fact, it has been known for some time that the real part of the K^-p scattering length extracted from the 1S level shift of the kaonic hydrogen atom and from $\bar{K}N$ scattering have opposite signs. A recent examination of this "kaonic hydrogen puzzle" by Tanaka and Suzuki [41]) using two different models seem to favor the one assuming a two-body composite system for the $\Lambda(1405)$.

In summary, with the exception of $\Lambda(1405)$, the chiral bag model describes the mass spectrum of the negative-parity hyperons reasonably well which, together with the earlier success of describing the N* and Δ* negative-parity mass spectrum [25,19]), makes this model a strong competitor to the NRQM. We have also calculated the partial and total hadronic widths of $\Lambda(1520)$ and find them to be close to the experimentally observed ones. Furthermore, we find that the electromagnetic decay widths of the two lightest excited hyperons in this model are much smaller than the ones calculated in the NRQM [4]). We stress that to understand the difference between the structures of $\Lambda(1520)$ and $\Lambda(1405)$ hyperons and the nature of their observed $\boldsymbol{L}\cdot\boldsymbol{S}$ splitting, both states, which are close to the $\bar{K}N$ threshold, should be examined within the same model.

We thank G.E. Brown for encouraging and inspiring this collaboration and Jim Lowe for numerous correspondences. One of us (Y.U.) would like to thank the University of South Carolina at Coulombia for kind hospitality.

Appendix A

HYPERON MASS CORRECTIONS

Here we discuss details regarding the estimates of the mass correction factor (i.e. the real part of $\delta_L(\mathrm{BB}')$) in eq. (4), which multiply the spin-flavor matrix elements of eq. (3). We apply this mass correction to $\Lambda(\frac{3}{2}^-)_3$ and $\Lambda(\frac{1}{2}^-)_3$ and discuss why our model gives the unexpected mass ordering of these two lightest excited hyperons as shown in fig. 1.

In eq. (4) we use the "bare" mass for the initial/final baryon state, m_{B}, which for $\mathrm{B}=\Lambda(\frac{3}{2}^-)_3$ and $\Lambda(\frac{1}{2}^-)_3$ are about equal and are approximately 1695 MeV. This "bare" mass value is not too different from what is needed in the calculations of Veit *et al.* [12]), Siegel and Weise [13]) and Arima and Yazaki [21]) and is a result of our bag-model calculation including all one-gluon exchange interaction terms, but excluding all meson-cloud contributions [7]). The "bare" ground-state baryon-octet masses taken from ref. [26]) are used for the intermediate baryon masses, $m_{\mathrm{B}'}$. In general, $m_{\mathrm{B}'}-m_{\mathrm{B}}=-\Delta<0$, which gives our "static" estimate for the mass corrections. When $\mathrm{B}=\Lambda(\frac{1}{2}^-)$, eq. (4) gives $\mathrm{Re}\,\delta_0(\Lambda(\frac{1}{2}^-)_3\mathrm{N})\approx 9$ for the $\bar{\mathrm{K}}\mathrm{N}$ $L=0$ intermediate state and the correction factor for the $\pi\Sigma$ intermediate state is $\mathrm{Re}\,\delta_0(\Lambda(\frac{1}{2}^-)_3\Sigma)\approx 3$. For $\mathrm{B}=\Lambda(\frac{3}{2}^-)$, we use the "non-static" estimate since the baryon recoil will be particularly important for the $\bar{\mathrm{K}}\mathrm{N}$ intermediate state with $L=2$. In this case, the corresponding correction factors are found to be $\mathrm{Re}\,\delta_2(\Lambda(\frac{3}{2}^-)_3\mathrm{N})\approx 5$ and $\mathrm{Re}\,\delta_2(\Lambda(\frac{3}{2}^-)_3\Sigma)\approx 4$ for the $L=2$ meson-baryon intermediate states. The value of the correction factor $\mathrm{Re}\,\delta_2(\Lambda(\frac{3}{2}^-)_3\mathrm{N})$ is very sensitive to the "bare" baryon mass difference $m_{\mathrm{B}'}-m_{\mathrm{B}}$ due to the closeness of the $\bar{\mathrm{K}}\mathrm{N}$ threshold and the $L=2$ centrifugal factor.

Using these correction factors in eq. (3), we find $\Lambda(\frac{3}{2}^-)_3$ to be lower in mass than $\Lambda(\frac{1}{2}^-)_3$ contradicting observations if we were to identify $\Lambda(1520)$ with $\Lambda(\frac{3}{2}^-)_3$ and $\Lambda(1405)$ with $\Lambda(\frac{1}{2}^-)_3$. The reasons are inherent in our model and are as follows. For $\Lambda(\frac{3}{2}^-)_3$, the $\bar{\mathrm{K}}\mathrm{N}$ and the $\pi\Sigma$ intermediate-state couplings in eq. (3) operates only through the $k^{\mathrm{K}}_{SA'A'S}$ and k^{π}_{SAAS} quadrupole transition operators [see table II of ref. [19])]. Here, as in sect. 2.2, A' denotes a massive s-quark in the $\mathrm{P}_{3/2}$ state. In our model calculations, the wave function for the lightest $J^P=\frac{3}{2}^-$ Λ^* state was found to be [7])

$$|\Lambda(\tfrac{3}{2}^-)_3\rangle=-0.95|^2 1_{3/2}\rangle-0.09|^4 8_{3/2}\rangle+0.29|^2 8_{3/2}\rangle \qquad \text{(A.1)}$$

which is clearly dominated by the flavor-singlet component. The pionic cloud

contribution to the $J^P = \frac{3}{2}^-$ states, H_π, is given by a 3×3 matrix defined by

$$H_\pi \equiv \begin{pmatrix} \langle {}^2 1_{3/2}|O_\pi|^2 1_{3/2}\rangle & \langle {}^2 1_{3/2}|O_\pi|^4 8_{3/2}\rangle & \langle {}^2 1_{3/2}|O_\pi|^2 8_{3/2}\rangle \\ \langle {}^4 8_{3/2}|O_\pi|^2 1_{3/2}\rangle & \langle {}^4 8_{3/2}|O_\pi|^4 8_{3/2}\rangle & \langle {}^4 8_{3/2}|O_\pi|^2 8_{3/2}\rangle \\ \langle {}^2 8_{3/2}|O_\pi|^2 1_{3/2}\rangle & \langle {}^2 8_{3/2}|O_\pi|^4 8_{3/2}\rangle & \langle {}^2 8_{3/2}|O_\pi|^2 8_{3/2}\rangle \end{pmatrix}, \tag{A.2}$$

where O_π is the effective-quark one-pion exhange interaction operator. The matrix in eq. (A.2) is similar to eq. (2) in ref. [7]). With a bag radius of 1.2 fm and strange quark mass of 250 MeV the matrix elements in H_π are (the numbers are in MeV)

$$H_\pi = \begin{pmatrix} -104 & -7 & 22 \\ -7 & -41 & 21 \\ 22 & 21 & -79 \end{pmatrix} \tag{A.3}$$

and the corresponding kaon-cloud contribution is

$$H_K = \begin{pmatrix} -34 & 1 & 2 \\ 1 & -25 & 7 \\ 2 & 7 & -30 \end{pmatrix}. \tag{A.4}$$

The intermediate baryon-octet ground states (with all three quarks in the S-state) contribute to the matrix elements in eqs. (A.3) and (A.4). The meson-cloud contributions to the octet components of $\Lambda(\frac{3}{2}^-)_3$ and $\Lambda(\frac{1}{2}^-)_3$ states keep these two lowest $J^P = \frac{3}{2}^-$ and $\frac{1}{2}^-$ states approximately mass degenerate. Therefore, in this discussion we shall concentrate on the contribution from the pure flavor-singlet component which is responsible for the unexpected mass ordering of the lowest $J^P = \frac{3}{2}^-$ and $\frac{1}{2}^-$ states.

The pure flavor-singlet mass contributions from the pion cloud, denoted as $\langle {}^2 1_{3/2}|O_\pi|^2 1_{3/2}\rangle$ in eq. (A.3), is -104 MeV. This contains a contribution from the $\pi\Sigma$ intermediate state of $5\mathrm{Re}\,\delta_2(\Lambda(\frac{3}{2}^-)_3\Sigma)k^\pi_{SAAS} = -16.6$ MeV when $\mathrm{Re}\,\delta_2(\Lambda(\frac{3}{2}^-)_3\Sigma) = 1$. Similarly, the kaon-cloud contribution to the flavor singlet is -34 MeV as shown in eq. (A.4) and this includes a $\bar{K}N$ intermediate state of contribution of $\frac{10}{3}\mathrm{Re}\,\delta_2(\Lambda(\frac{3}{2}^-)_3\mathrm{N})k^K_{SA'A'S} = -3.73$ MeV when $\mathrm{Re}\,\delta_2(\Lambda(\frac{3}{2}^-)_3\mathrm{N}) = 1$. The corresponding contributions to the flavor-singlet component of $\Lambda(\frac{1}{2}^-)_3$ are as follows [see e.g. eq. (2c) in ref. [7])]. For the pion cloud we have a contribution of -62 MeV which includes an intermediate $\pi\Sigma$ state contribution of $2\mathrm{Re}\,\delta_0(\Lambda(\frac{1}{2}^-)_3\Sigma)m^\pi_{SPPS} = -8.7$ MeV when $\mathrm{Re}\,\delta_0(\Lambda(\frac{1}{2}^-)_3\Sigma) = 1$, and the kaon-cloud mass contribution is -13 MeV of which the $\bar{K}N$ intermediate-state contribution is $4\mathrm{Re}\,\delta_0(\Lambda(\frac{1}{2}^-)_3\mathrm{N})m^K_{SP'P'S} = -1.85$ MeV when $\mathrm{Re}\,\delta_0(\Lambda(\frac{1}{2}^-)_3\mathrm{N}) = 1$. We note that when we calculate the spin-flavor matrix elements between the various baryon states we use the prescription of ref. [25]), (see fig. 4 of this reference) where the quark remains in its initial state when $i = j$ in the sum over the quark indices i and j in eq. (3). The consequence of this prescription is that only the terms $i \neq j$ in eq. (3) contribute to the $\pi\Sigma$ and $\bar{K}N$ intermediate states. (We relax this restriction when we calculate the hadronic widths of the hyperons in sect. 2.3 of this paper.)

Assuming now that $\Lambda(\frac{3}{2}^-)_3$ and $\Lambda(\frac{1}{2}^-)_3$ are pure flavor singlets, we find, with no mass correction factors (i.e., with all Re $\delta_L(\mathrm{BB}')=1$), the following masses:

$$M_{\Lambda(\frac{3}{2}^-)_3} = (1695-104-34)\ \mathrm{MeV} = 1557\ \mathrm{MeV}, \tag{A.5}$$

$$M_{\Lambda(\frac{1}{2}^-)_3} = (1695-62-13)\ \mathrm{MeV} = 1620\ \mathrm{MeV}. \tag{A.6}$$

Here the three terms in the parentheses are the "bare" Λ^* mass, the pion- and the kaon-cloud contributions, respectively. When we include the estimated values of the real part of the mass correction factors quoted above, we find the following changes to the above masses:

$$M_{\Lambda(\frac{3}{2}^-)_3} = (1695-154-49)\ \mathrm{MeV} = 1492\ \mathrm{MeV}, \tag{A.7}$$

$$M_{\Lambda(\frac{1}{2}^-)_3} = (1695-79-43)\ \mathrm{MeV} = 1573\ \mathrm{MeV}. \tag{A.8}$$

Although the mass correction factors for the $\bar{\mathrm{K}}\mathrm{N}$ intermediate states are all very large, the kaon-cloud contributions are too small to invert the calculated mass ordering. The reason is due to the small values of the kaon-cloud transition matrix elements, $k^{\mathrm{K}}_{SA'A'S}$ and $m^{\mathrm{K}}_{SP'PS}$, a result of the heavy kaon mass. It seems to be necessary to go beyond lowest order of this model, perhaps by including the non-perturbative effects of the meson cloud, to explain the mass splitting of the $\Lambda(1520)$ and $\Lambda(1405)$. Note that in the cloudy bag model of Veit *et al.* [12]) an additional, very attractive, four-point quark–meson interaction of the type $\bar{q}\gamma^\mu q(\phi \times \partial_\mu \phi)$, which is second order in the meson field, is included leading to a $L=0$ meson–baryon contact interaction. The effect of this interaction term on the $\Lambda(1520)$ state should be examined.

Appendix B

YK̄N COUPLING CONSTANTS

In this appendix we briefly present the calculation of the hyperon coupling constants $G_{\Lambda\bar{\mathrm{K}}\mathrm{N}}$ and $G_{\Sigma^0\bar{\mathrm{K}}\mathrm{N}}$ in the chiral bag model where the meson cloud is treated as a perturbation. The method employed in determining $G_{\mathrm{Y}\bar{\mathrm{K}}\mathrm{N}}$ is a straightforward generalization of the calculation of πNN coupling constant as described in ref. [24]). The basic assumption made here is the identification of the hyperon coupling constant $G_{\mathrm{Y}\bar{\mathrm{K}}\mathrm{N}}$ with the usual πNN coupling constant in the SU(3) limit (i.e. the s-quark mass equals the u- and d-quark masses *and* the kaon mass becomes equal to the pion mass).

If the quark-meson coupling at the bag surface is linearized as in eq. (1), then the K^- field generated by a strange quark in the S-state can be written as

$$K^-(\boldsymbol{r}) = -\frac{A(-1)N(-1)}{4\pi f_K}\frac{\mu^2 e^{\mu R}}{(\mu R+1)^2+1}\frac{1+\mu r}{(\mu r)^2}e^{-\mu r}\left\langle \sum_i \boldsymbol{\sigma}(i)V_+(i)\right\rangle\cdot\hat{\boldsymbol{r}} \quad \text{(B.1)}$$

where $r \geqslant R$. Here μ is the kaon mass, f_K is the kaon decay constant and the quark index i runs from 1 to 3. V_+ is the V-spin raising operator acting on the flavor wavefunction. The coefficients $A(-1)$ and $N(-1)$ are proportional to the normalization constants for the s-quark and u- or d-quark wavefunctions in the bag cavity, respectively, so that in the SU(3) limit $A(-1) \to N(-1)$. In close analogy with the calculation of πNN coupling constant, *define* the quark-kaon coupling constant g_{qK} as

$$\frac{g_{qK}}{M} \equiv \frac{A(-1)N(-1)}{f_K}\frac{e^{\mu R}}{(\mu R+1)^2+1} \quad \text{(B.2)}$$

so that the K^- field outside the bag becomes

$$K^-(\boldsymbol{r}) = -\frac{\mu^2}{4\pi}\frac{g_{qK}}{M}\frac{1+\mu r}{(\mu r)^2}e^{-\mu r}\left\langle \sum_i \boldsymbol{\sigma}(i)V_+(i)\right\rangle\cdot\hat{\boldsymbol{r}}. \quad \text{(B.3)}$$

In eq. (B.2), M is the nucleon mass and in the SU(3) limit g_{qK} reproduces the quark-pion coupling constant discussed in ref. [24]).

The coupling constant for the Λ and Σ^0 hyperons are determined by relating the expectation value of the quark operator $\Sigma_i \boldsymbol{\sigma}(i)V_+(i)$ between the relevant baryon states to that evaluated at the meson-baryon level. For example let

$$\langle p\uparrow|\sum_i \boldsymbol{\sigma}(i)V_+(i)|\Lambda\uparrow\rangle = aU_N^\dagger \boldsymbol{\sigma} V_+ U_\Lambda\,, \quad \text{(B.4)}$$

where $\uparrow$ indicates "spin up" and U_Λ and U_N are the Pauli spinors for Λ and the nucleon, respectively. Then the magnitude of the physical $\Lambda\bar{K}N$ coupling constant, denoted as $G_{\Lambda\bar{K}N}$ in sect. 2.3, is given by

$$|G_{\Lambda KN}| = a|g_{qK}|\,. \quad \text{(B.5)}$$

A standard calculation gives

$$|g_{qK}| = \begin{cases}\sqrt{\frac{1}{2}}|G_{\Lambda KN}| \\ 3\sqrt{\frac{1}{2}}|G_{\Sigma^0 KN}|\,.\end{cases} \quad \text{(B.6)}$$

The value of the quark-kaon coupling constant is a function of the strange quark mass and the bag radius. With $m_S = 250$ MeV and $R = 1.125$ fm, $|g_{qK}|$ is found to be 6.84 and the resulting magnitude of the physical $\Lambda\bar{K}N$ and $\Sigma^0\bar{K}N$ coupling constants are 9.68 and 3.23, respectively.

Appendix C

MESON ELECTROMAGNETIC CURRENTS

In this appendix we outline a derivation of pion electromagnetic transition currents and their corresponding radial integrals used to evaluate the meson-cloud contributions to the hyperon radiative decay widths. Let $\pi_{XY}(\boldsymbol{r})$ be the effective pion field emitted by a quark at the bag surface in an initial state X and final state Y, where X and Y can be in any of quark states $S \equiv S_{1/2}$, $P \equiv P_{1/2}$ or $A \equiv P_{3/2}$. As discussed these pion fields are determined by requiring a continuous axial current across the bag surface in the chiral limit, and their derivation was presented explicitly in appendix A of ref. [19]). The general expression for the pion field is

$$\pi_{XY} \equiv \boldsymbol{\pi}_{XY}(\boldsymbol{r}) = \frac{i}{2f_\pi} \sum_{l,m} f_l(i\mu r) \int d^2r' \, (\bar{q}x(\boldsymbol{r}')\gamma_5 \boldsymbol{\tau} q_Y(\boldsymbol{r}'))|_{r'=R} \, Y^*_{lm}(\hat{\boldsymbol{r}}) \, Y_{lm}(\hat{\boldsymbol{r}}') \,, \tag{C.1}$$

where

$$f_l(i\mu r) \equiv \frac{h_l(i\mu r)}{\partial h_l(i\mu R)/\partial R} \tag{C.2}$$

and $h_l(x)$ are the spherical Hankel functions of the first kind

$$h_l(x) = -i(-1)^l x^l \left(\frac{1}{x}\frac{d}{dx}\right)^l \left(\frac{e^{ix}}{x}\right). \tag{C.3}$$

Here $q_Y(\boldsymbol{r})$ is the field of a quark in state Y, μ is the pion mass and $Y_{lm}(\hat{\boldsymbol{r}})$ is the spherical harmonic.

The pion electromagnetic transition current can easily be constructed from the model lagrangian given in eq. (1). Let $\boldsymbol{J}^{ij}_\pi(XYZW)$ be the pion transition current emitted by a quark i in an initial state X and final state Y and absorbed by a quark j in an initial state Z and final state W (see fig. C.1a). Then $\boldsymbol{J}^{ij}_\pi(XYZW)$, which in sect. 3 is defined generically as J_m, can be written as

$$\boldsymbol{J}^{ij}_\pi(XYZW) = -\tfrac{1}{2}ie[(\nabla \pi^i_{XY})^\dagger \pi^j_{ZW} - (\pi^i_{XY})^\dagger \nabla \pi^j_{ZW}] \,. \tag{C.4}$$

Since these pion fields are solutions of the Klein-Gordon equation, the pion electromagnetic current $\boldsymbol{J}^{ij}_\pi$ is automatically conserved. For example, using the notation of ref. [25]), the transition currents corresponding to the diagrams in figs. C.1b and C.1c are

$$\begin{aligned} \boldsymbol{J}^{ij}_\pi(PSSS) &= -\tfrac{1}{2}ie[(\nabla \pi^i_{PS})^\dagger \pi^j_{SS} - (\pi^i_{PS})^\dagger \nabla \pi^j_{SS}] \\ &= +\tfrac{1}{2}ieT_+(i)\,T_-(j)\left(\frac{N(S)^3 N(P)}{16\pi^2 f_\pi^2}\right) P^i[P \to S] \\ &\quad \times \frac{1}{r}[g_1(i\mu r)\boldsymbol{\sigma}(j)\cdot\hat{\boldsymbol{r}}\boldsymbol{r} - f_0(i\mu r) f_1(i\mu r)\boldsymbol{\sigma}(j)] \end{aligned} \tag{C.5}$$

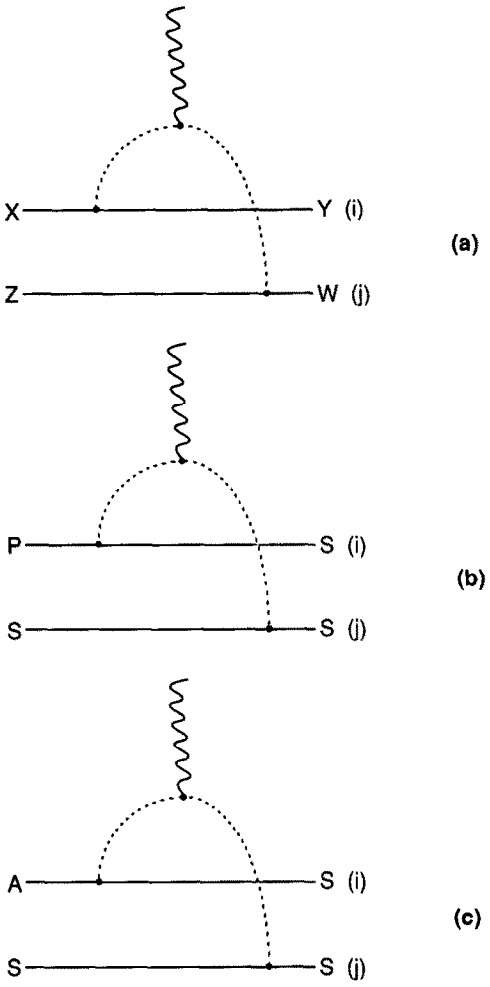

Fig. C.1. (a): A typical diagram involving the meson electromagnetic transition current. Here the quark i (solid line) emits a meson (dashed line) and changes its state from X to Y. The emitted meson radiates a photon (wiggly line) and is subsequently absorbed by the quark j which changes its state from Z to W. (b): The diagram involving the pion electromagnetic transition current $J^{ij}_{\pi}(PSSS)$ of eq. (C.5). Here the dashed line represents a pion in flight. (c): The corresponding diagram involving the current $J^{ij}_{\pi}(ASSS)$ of eq. (C.6). See appendix C for details of their derivations.

and

$$J^{ij}_{\pi}(ASSS) = -\tfrac{1}{2}ie[(\nabla\pi^{i}_{AS})^{\dagger}\pi^{j}_{SS} - (\pi^{i}_{AS})^{\dagger}\nabla\pi^{j}_{SS}]$$

$$= +\tfrac{1}{2}ieT_{+}(i)T_{-}(j)\left(\frac{N(S)^3N(A)}{8\sqrt{6}\pi^2 f_{\pi}^2}\right)K_{ab}^{[3/2,1/2]}(i)$$

$$\times\frac{1}{r}[f_1(i\mu r)f_2(i\mu r)(\boldsymbol{\sigma}(j)\hat{\mathbf{r}}_a\hat{r}_b - \sigma_c(j)\hat{r}_a\hat{r}_c\hat{e}_b)$$

$$+ g_2(i\mu r)\sigma_c(j)\hat{r}_a\hat{r}_b\hat{r}_c\hat{r}]\,. \qquad \text{(C.6)}$$

Here the isospin operator $T_{\pm} \equiv \mp\sqrt{\frac{1}{2}}(\lambda_1 \pm i\lambda_2)$ and λ_i are the 3×3 Gell-Mann matrices in flavor space. The subscripts $a, b, c = 1, 2, 3$ indicate the cartesian components of the vectors or tensors and $\hat{e}$ is a spacial unit vector. The permutation operator $P^i[X \to Y]$ permutes the states X and Y of quark i, the components of the vector $\boldsymbol{\sigma}$ are the usual Pauli spin matrices and $K_{ab}^{[3/2,1/2]}$ is a quadrupole transition operator defined in ref. [25]). The function $g_n(i\mu r)$ is given by

$$g_n(i\mu r) = f_n(i\mu r)\left(\frac{\mathrm{d}f_{n-1}(i\mu r)}{\mathrm{d}r} - (n-1)\frac{f_{n-1}(i\mu r)}{r}\right)$$

$$-f_{n-1}(i\mu r)\left(\frac{\mathrm{d}f_n(i\mu r)}{\mathrm{d}r} - n\frac{f_n(i\mu r)}{r}\right). \tag{C.7}$$

It is evident that the transition operators resulting from these two currents are two-body operators in quark space and no other currents need to be constructed if one allows only ground-state baryons as intermediate baryon states.

Volume integrals needed to evaluate I_m in eq. (7) are straightforward but lengthy. In the following equations, the photon polarization vector $\hat{\boldsymbol{\varepsilon}}$ is expressed in cartesian coordinates, i.e. $\hat{\boldsymbol{\varepsilon}}_1 \equiv (1, 0, 0)$ and $\hat{\boldsymbol{\varepsilon}}_2 \equiv (0, 1, 0)$. For $P \to S$ transitions, the volume integral using the pion electromagnetic current of eq. (C.5) is

$$\hat{\boldsymbol{\varepsilon}}_l \cdot \int_R^\infty \mathrm{d}^3 r \boldsymbol{J}_\pi^{ij}(PSSS)\, \mathrm{e}^{-i\boldsymbol{k}\cdot\boldsymbol{r}} = +\tfrac{1}{2}ieT_+(i)T_-(j)\left(\frac{N(S)^3N(P)}{16\pi^2 f_\pi^2}\right)P^i[P\to S]$$

$$\times\left[i\tfrac{4}{3}\pi\frac{R}{\mu}H_0(i\mu R)H_1(i\mu R)(I_1 - I_2)\right]\sigma_l(j)\,. \tag{C.8}$$

Here the subscript l for $\hat{\boldsymbol{\varepsilon}}$ and σ is either 1 or 2. The volume integrals for $A \to S$ transitions involving the current in eq. (C.6) have a more complicated operator structure:

$$\hat{\boldsymbol{\varepsilon}}_1 \cdot \int_R^\infty \mathrm{d}^3 r \boldsymbol{J}_\pi^{ij}(ASSS)\, \mathrm{e}^{-i\boldsymbol{k}\cdot\boldsymbol{r}}$$

$$= +\tfrac{1}{2}ieT_+(i)T_-(j)\left(\frac{N(S)^3N(A)}{8\sqrt{6}\pi^2 f_\pi^2}\right)$$

$$\times\left(i4\pi\frac{R}{\mu}H_1(i\mu R)H_2(i\mu R)\right)[(A(\mu R)K_{11}^{[3/2,1/2]}(i)$$

$$+B(\mu R)K_{22}^{[3/2,1/2]}(i) + C(\mu R)K_{33}^{[3/2,1/2]}(i))\sigma_1(j)$$

$$+D(\mu R)K_{12}^{[3/2,1/2]}(i)\sigma_2(j) + E(\mu R)K_{13}^{[3/2,1/2]}(i)\sigma_3(j)]\,, \tag{C.9}$$

$$\hat{\varepsilon}_2 \cdot \int_R^\infty \mathrm{d}^3 r \, \boldsymbol{J}_\pi^{ij}(ASSS)\, \mathrm{e}^{-i\boldsymbol{k}\cdot\boldsymbol{r}}$$

$$= +\tfrac{1}{2} ieT_+(i)T_-(j)\left(\frac{N(S)^3 N(A)}{8\sqrt{6}\pi^2 f_\pi^2}\right)$$

$$\times\left(i4\pi \frac{R}{\mu} H_1(i\mu R)H_2(i\mu R)\right)[D(\mu R)K_{12}^{[3/2,1/2]}(i)\sigma_1(j)$$

$$+(A(\mu R)K_{11}^{[3/2,1/2]}(i)+B(\mu R)K_{22}^{[3/2,1/2]}(i)$$

$$+C(\mu R)K_{33}^{[3/2,1/2]}(i))\sigma_2(j)+E(\mu R)K_{23}^{[3/2,1/2]}(i)\sigma_3(j)]\,. \qquad \text{(C.10)}$$

The function $H_n(i\mu R)$ is defined as

$$H_n(i\mu R) \equiv i\mu\left[\frac{n}{i\mu R} h_n(i\mu R) - h_{n+1}(i\mu R)\right] \qquad \text{(C.11)}$$

and the coefficients $A(\mu R)$ through $E(\mu R)$ are given by

$$A(\mu R) = +\tfrac{1}{3} I_3 - \tfrac{5}{21} I_4 - \tfrac{2}{35} I_5 - \tfrac{2}{35} I_6\,, \qquad \text{(C.12)}$$

$$B(\mu R) = -\tfrac{1}{3} I_3 - \tfrac{1}{21} I_4\,, \qquad \text{(C.13)}$$

$$C(\mu R) = +\tfrac{2}{3} I_3 + \tfrac{2}{21} I_4 + \tfrac{1}{7} I_5\,, \qquad \text{(C.14)}$$

$$D(\mu R) = +\tfrac{2}{3} I_3 - \tfrac{4}{21} I_4 - \tfrac{2}{35} I_5 + \tfrac{2}{35} I_6\,, \qquad \text{(C.15)}$$

$$E(\mu R) = -\tfrac{4}{3} I_3 + \tfrac{2}{21} I_4 + \tfrac{8}{35} I_5 + \tfrac{2}{35} I_6\,, \qquad \text{(C.16)}$$

where

$$I_1 = \int_1^\infty \mathrm{d}x\, j_0(kRx)\left(\frac{2}{\mu Rx} + \frac{1}{(\mu Rx)^2}\right)\mathrm{e}^{-2\mu Rx}\,, \qquad \text{(C.17)}$$

$$I_2 = \int_1^\infty \mathrm{d}x\, j_2(kRx)\left(\frac{1}{\mu Rx} + \frac{2}{(\mu Rx)^2}\right)\mathrm{e}^{-2\mu Rx}\,, \qquad \text{(C.18)}$$

$$I_3 = \int_1^\infty \mathrm{d}x\, j_2(kRx)\left(\frac{1}{\mu Rx} + \frac{4}{(\mu Rx)^2} + \frac{6}{(\mu Rx)^3} + \frac{3}{(\mu Rx)^4}\right)\mathrm{e}^{-2\mu Rx}\,, \qquad \text{(C.19)}$$

$$I_4 = \int_1^\infty \mathrm{d}x\, j_2(kRx)\left(\frac{1}{\mu Rx} + \frac{6}{(\mu Rx)^2} + \frac{12}{(\mu Rx)^3} + \frac{6}{(\mu Rx)^4}\right)\mathrm{e}^{-2\mu Rx}\,, \qquad \text{(C.20)}$$

$$I_5 = \int_1^\infty \mathrm{d}x\, j_4(kRx)\left(\frac{1}{\mu Rx} + \frac{6}{(\mu Rx)^2} + \frac{12}{(\mu Rx)^3} + \frac{6}{(\mu Rx)^4}\right)\mathrm{e}^{-2\mu Rx}\,. \qquad \text{(C.21)}$$

$$I_6 = \int_1^\infty \mathrm{d}x\, j_0(kRx)\left(\frac{4}{\mu Rx} + \frac{14}{(\mu Rx)^2} + \frac{18}{(\mu Rx)^3} + \frac{9}{(\mu Rx)^4}\right) \mathrm{e}^{-2\mu Rx}. \qquad \text{(C.22)}$$

Corresponding expressions for kaon electromagnetic transition currents may be derived in a similar manner with an appropriate substitution of the isospin operator $T_\pm$ by the V-spin operator $V_\pm \equiv \mp\sqrt{\frac{1}{2}}(\lambda_4 \pm i\lambda_5)$.

References

1) P.D. Barnes *et al.*, Electromagnetic production of hyperons, CEBAF Letter of Intent (unpublished)
2) H. Pilkuhn, *in* The interactions of hadrons (North-Holland, Amsterdam, 1967)
3) Particle Data Group, Phys. Rev. **D45** (1992) part II
4) J.W. Darewych, M. Horbatsch and R. Koniuk, Phys. Rev. **D28** (1983) 1125
5) M. Warns, W. Pfeil and H. Rollnik, Phys. Lett. **B258** (1991) 431
6) E. Kaxiras, E.J. Moniz and M. Soyeur, Phys. Rev. **D32** (1985) 695
7) Y. Umino and F. Myhrer, Nucl. Phys. **A529** (1991) 713
8) D.L. Adams, *et al.*, Radiative decays of low-lying hyperons, CEBAF Letter of Intent (unpublished)
9) N. Isgur and G. Karl, Phys. Rev. **D18** (1978) 4187
10) F. Close, *in* An introduction to quarks and partons (Academic Press, New York, 1979)
11) T. DeGrand and R.L. Jaffe, Ann. of Phys. **100** (1976) 425;
    T. DeGrand, Ann. of Phys. **101** (1976) 496
12) E.A. Veit, B.K. Jennings, R.C. Barrett and A.W. Thomas, Phys. Lett. **B137** (1984) 415;
    E.A. Veit, B.K. Jennings, A.W. Thomas and R.C. Barrett, Phys. Rev. **D31** (1985) 1033
13) P.B. Siegel and W. Weise, Phys. Rev. **C38** (1988) 2221
14) P.J. Fink, G. He, R.H. Landau and J.W. Schnick, Phys. Rev. **C41** (1990) 2720
15) C.G. Callen, K. Hornbostel and I. Klebanov, Phys. Lett. **B202** (1988) 269;
    C.G. Callen and I. Klebanov, Nucl. Phys. **B262** (1985) 365
16) R.H. Dalitz, Rev. Mod. Phys. **33** (1961) 471
17) G.C. Oades and G. Rasche, Nuovo Cim. **42A** (1977) 462; Phys. Scr. **26** (1982) 15
18) R.A. Williams, C.-R. Ji and S.R. Cotanch, Phys. Rev. **C43** (1991) 452
19) Y. Umino and F. Myhrer, Phys. Rev. **D39** (1989) 3391
20) N.A. Törnqvist and P. Zenczykowski, Z. Phys. **C30** (1986) 83
21) M. Arima and K. Yazaki, Nucl. Phys. **A506** (1990) 553
22) B. Silvestre-Brac and C. Gignoux, Phys. Rev. **D43** (1991) 3699
23) S.K. Sharma *et al.*, Phys. Rev. Lett. **62** (1989) 2913;
    W. Blask *et al.*, Z. Phys. **A326** (1987) 413
24) F. Myhrer, *in* International review of nuclear physics, ed. W. Weise, vol. 1 (World Scientific, Singapore 1984) p. 326
25) J. Wroldsen and F. Myhrer, Z. Phys. **C25** (1984) 59;
    F. Myhrer and J. Wroldsen, Z. Phys. **C25** (1984) 281
26) F. Myhrer, G.E. Brown and Z. Xu, Nucl. Phys. **A362** (1981) 317;
    F. Myhrer and Z. Xu, Phys. Lett. **B108** (1982) 372
27) R.L. Jaffe, Phys. Rev. **D21** (1980) 3215
28) R.H. Dalitz and A. Deloff, J. of Phys. **G17** (1991) 289
29) O. Dumbrajs *et al.*, Nucl. Phys. **B216** (1983) 277
30) M.M. Nagels *et al.*, Nucl. Phys. **B109** (1976) 1
31) R.A. Adelseck and B. Saghai, Phys. Rev. **C42** (1990) 108
32) C. Gobbi, D.O. Riska and N.N. Scoccola, Nucl. Phys. **A544** (1992) 671
33) Y.S. Zhong, A.W. Thomas, B.K. Jennings and R.C. Barrett, Phys. Lett. **B171** (1986) 471; Phys. Rev. **D38** (1988) 837
34) J. Kunz, P.J. Mulders and G.A. Miller, Phys. Lett. **B255** (1991) 11
35) G.E. Brown and M. Rho, Phys. Lett. **B82** (1979) 177

36) U. Blom, K. Dannbom and D.O. Riska, Nucl. Phys. **A493** (1989) 384;
K. Dannbom, E. Nyman and D.O. Riska, Phys. Lett. **B227** (1989) 291;
N.N. Scoccola, Phys. Lett. **B236** (1990) 245
37) Y. Umino, in preparation
38) H. Burkhardt and J. Lowe, Phys. Rev. **C44** (1991) 607
39) D.A. Whitehouse *et al.*, Phys. Rev. Lett. **63** (1989) 1352
40) J. Lowe, private communication
41) K. Tanaka and A. Suzuki, Phys. Rev. **C45** (1992) 2068